IranJOC

Iranian Journal of Organic Chemistry

Investigation of swelling and antibacterial properties of carboxymethyl chitosan/Poly (vinyl alcohol) nanocomposite hydrogels containing CuO nanoparticles

Iman Gholamali[a], Manzarbanou Asnaashariisfahani[a,*], Eskandar Alipour[a] and Abbas Akhavan Sepahi[b]

[a]*Department of Chemistry, North Tehran Branch, Islamic Azad University, P.O. Box 19585/936, Tehran, Iran*
[b]*Department of Microbiology, Faculty of Science, North Tehran Branch, Islamic Azad University, Tehran, Iran*

Abstract: The CsMe/PVA/CuO nanocomposite hydrogels have been introduced a new technique, which is dependent on pH. They were prepared successfully *in-situ* by forming of CuO nanoparticles within swollen CsMe/PVA hydrogels. The resulting hydrogels were examined by running various experimental procedures such as Fourier Transform Infrared Spectroscopy (FT-IR), X-ray diffraction patterns (XRD), Energy-dispersive X-ray spectroscopy (EDX) and Scanning electron microscopy (SEM). XRD and EDX patterns verified the formation of CuO nanoparticles in the hydrogel networks; moreover, the formation of CuO nanoparticles with size range from 13.89 to 47.78 nm within the hydrogel matrix was confirmed by SEM micrographs. The prepared nanocomposite hydrogels showed a pH-sensitive swelling behavior. The results showed that the prepared nanocomposite hydrogels outperformed the pure CsMe/PVA hydrogels in terms of swelling capacity in various pH values and salt solutions. The antibacterial activity of the nanocomposite hydrogels was examined and mechanisms involved in their synthesis were reported; the results showed an excellent antibacterial behavior of the nanocomposite hydrogels.

Introduction

Hydrogels are a class of materials with the three-dimensional network of a polymer that can absorb a high amount of water or biological fluids, without being soluble under physiological conditions [1]. Also, due to their excellent properties, such as high swelling ratio, non-toxicity, biocompatibility and biodegradability hydrogels would have basic roles in agriculture [2, 3], and biomedical applications including wound dressing [4], tissue engineering [5, 6] and controlled drug and protein delivery [7].

Chitosan is one of the most abundant natural cationic polymers produced commercially by deacetylation of chitin. Due to its unique poly-cationic nature, it has been widely applied in medical and pharmaceutical fields [9, 10]. Carboxymethyl chitosan (CsMe) is a biodegradable and biocompatible polymer obtained from the reaction of chitosan with mono-chloroacetic acid and in an alkaline medium [11]. CsMe has several advantages over chitosan such as increased water solubility, increased antioxidant property [12] high moisture retention ability [13] and higher antibacterial activity [9, 14] that Wahid et al. prepared and characterized antibacterial CsMe/ZnO nanocomposite hydrogels by *in-situ* formation of ZnO nanoparticles in

Corresponding author: Tel: 0098-8633677201-9; Fax: 0098-8633677203, E-mail: *m_Asnaashari@iau-tnb.ac.ir*

CsMe hydrogel matrix. Therefore, carboxymethylation of chitosan is a promising approach in a number of environmental, biomedical, and pharmaceutical applications [15, 16]. Poly (Vinyl Alcohol) (PVA) is a water soluble polymer, which has been studied intensively due to its excellent chemical stability, easy preparation, film-forming ability, biocompatibility, gel forming and physical properties [17-19]. PVA hydrogels are relevant for biomaterial and pharmaceutical applications such as drug delivery, wound dressing, contact lenses, and artificial organs [20, 21] that Ahmadian et al. studied on synthesis of PVA/CuO nanocomposite hydrogels applicable in a drug delivery system. Agnihotri et al. studied the chemical crosslinking of chitosan with a polymer owning to good chemical resistance, greater mechanical strength and hydrophilicity including PVA that may lead to the formation of a hydrogel composite for antibacterial applications [22]. Recently, there has been a great interest to generate antibacterial hydrogels because of their superior biomedical relevance [23]. Among antibacterial hydrogels, inorganic-based nanocomposite hydrogels are particularly promising for bacterial inactivation applications in materials and engineering science. These antibacterial agents possess a great potential to inhibit microbial growth. Because of they are easily functionalized with inorganic materials and biocompatible, this characteristic makes them attractive in the biomedical and biotechnological fields [15, 16]. Among them, silver based materials are of special interest owing to their broad spectrum inhibitory and strong bactericidal effect [24]. During the last few years, there has been an increased interest in silver nanocomposite hydrogels as an antimicrobial agent in the medical field [25-28]. Nanocomposites are a combination of biopolymers and inorganic materials, mainly metals like silver, copper, TiO_2, and ZnO in nano-dimensions. Superior mechanical strength, high thermal resistance and low permeability against gases and water vapor are a number of the properties of bio-nanocomposites. In recent years, bio-nanocomposites have been used as wound dressings and tissue engineering as well [29-31]. The main advantage using inorganic nanoparticles accompanied with the organic antimicrobial mediators are their strength, stability, and extended shelf life; besides, they can be used potentially for biomedical field [32].

Considering these facts, the objective of this study was to prepare and characterize a group of carboxymethyl chitosan/Poly (vinyl alcohol) hydrogels containing CuO nanoparticles. Novel CsMe/PVA/CuO nanocomposite hydrogels were successfully prepared by *in-situ* formation of CuO nanoparticles in the CsMe/PVA hydrogel matrix. The resulting nanocomposite hydrogels were characterized using FT-IR, XRD, EDX and SEM analyses. The effect of the concentration of the CuO nanoparticles on the swelling in different aqueous mediums and antibacterial activity for the Gram-negative *E. coli* and Gram-positive *S. aureus* bacteria was investigated.

Result and Discussion

FT-IR analysis

Figure **1a** displays the characteristic absorption peaks of the four components; CsMe, PVA and CuO nanoparticles. The FT-IR spectrum of the CsMe, a broad peak 3407 cm^{-1} is related to the stretching vibrations of –NH and –OH functional groups [34, 35]. Also, FT-IR spectrum of CsMe includes several peaks at 1591, 1410 and 1121 cm^{-1} related to C-O stretching and the bending modes of the N-H, C-N stretching and C-OH stretching on the polysaccharide skeleton, respectively [29]. The FT-IR spectrum of the PVA, a broad peak 3345 cm^{-1} is related to hydroxyl groups and several peaks at 2921 cm^{-1} is associated to C-H stretching of CH_2, 1416 cm^{-1} and 1100 cm^{-1} is related to CH_2 Scissoring and C-O stretching. FT-IR spectrum of CuO nanoparticles includes absorption peaks at 540 cm^{-1} associated to CuO stretching.

Figure **1b** showed FT-IR spectra of the pure CsMe/PVA hydrogel and CsMe/PVA/CuO nanocomposite hydrogel. In Figure, it is showed that the peaks absorption of O-H at 3417 cm^{-1} and 3334 cm^{-1} are attributed to intramolecular hydrogen bond pure hydrogel and nanocomposite hydrogel. Compared with the FT-IR spectra of pure CsMe/PVA hydrogel, CsMe/PVA/CuO nanocomposite hydrogel indicated the new peaks in the 400-800 cm^{-1} regions. These peaks were attributed to the incorporation of metal bonds into the hydrogel.
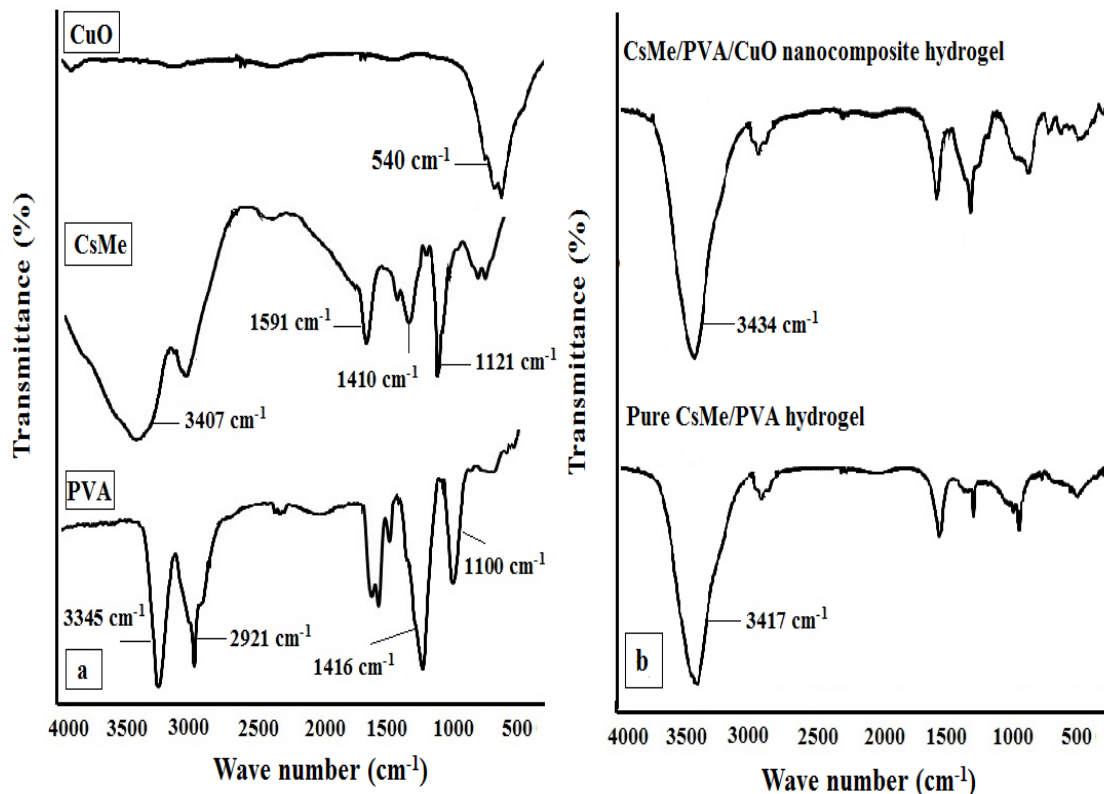
Figure. 1: FT-IR spectra of (a) pure CsMe, PVA and CuO nanoparticles; (b) pure CsMe/PVA hydrogel and CsMe/PVA/CuO nanocomposite hydrogel.

XRD analysis

The XRD patterns of the CsMe/PVA/CuO nanocomposite hydrogel and pure CsMe/PVA hydrogel in the 2θ range of 2-70° are shown in Figure **2**. The diffractogram of CsMe/PVA/CuO nanocomposite hydrogel is assigned to diffractions at 2θ values four peaks of 31°, 33°, 36° and 52° planes. All the peaks match well with those of monoclinic phase CuO crystals and confirm the formation of CuO nanoparticles in the CsMe/PVA hydrogel matrix. None of other peaks can be observed in the XRD pattern that indicates the high purity of obtained CuO particles [1, 37]. A wide peak at 20° is due to the polymer networks with the proposed structure. The IR spectrum of compound **4c** also supported the suggested structure.

Although we didn't study the mechanism of the reaction, but a reasonable possibility is presented in Scheme **2**. As can be seen from this Scheme, firstly, Knoevenagel condensation between Meldrum's acid and aldehyde will occur and arylidene Meldrum's acid **5** is formed. From Michael type nucleophilic attack of intermediate **6** (that was obtained from the reaction of 2-hydroxy-1,4-naphthoquinone with piperidine) to arylidene Meldrum's acid **5**, intermediate **7** was obtained.

Scanning electron microscopy (SEM) and Energy dispersive X-ray spectroscopy (EDX)

Scanning electron microscopy (SEM) was employed for investigation of the surface morphology of the samples, shape, size and porosity of the hydrogel matrices. SEM of the pure hydrogel and CsMe/PVA/CuO nanocomposite hydrogel at ×100,000 magnification are given in Figure **3**. The morphological of surface of the pure CsMe/PVA hydrogel indicated numerous wrinkles and several cavities because the hydrogel network collapsed

incompletely during drying. The nanocomposite hydrogels of CsMe/PVA/CuO showed a smooth and uniform surface morphology. These results seemed due to interfacial interactions of CuO nanoparticles with the CsMe/PVA macromolecules that the CuO nanoparticles could contract and hinder the movability of the CsMe/PVA chains, then changing the surface morphology. After examining the hydrogels, the nanoparticles were observed more clearly on the surface of the nanocomposite hydrogels including 0.5% CuO nanoparticles content with the particle size range was between 13.89 and 21.82 nm (sample Cu1) and some aggregation and bigger particle sizes (35.59-47.78 nm) can be seen for the CsMe/PVA/CuO nanocomposite hydrogels containing the highest copper chloride concentration of 1.5% (sample Cu3).
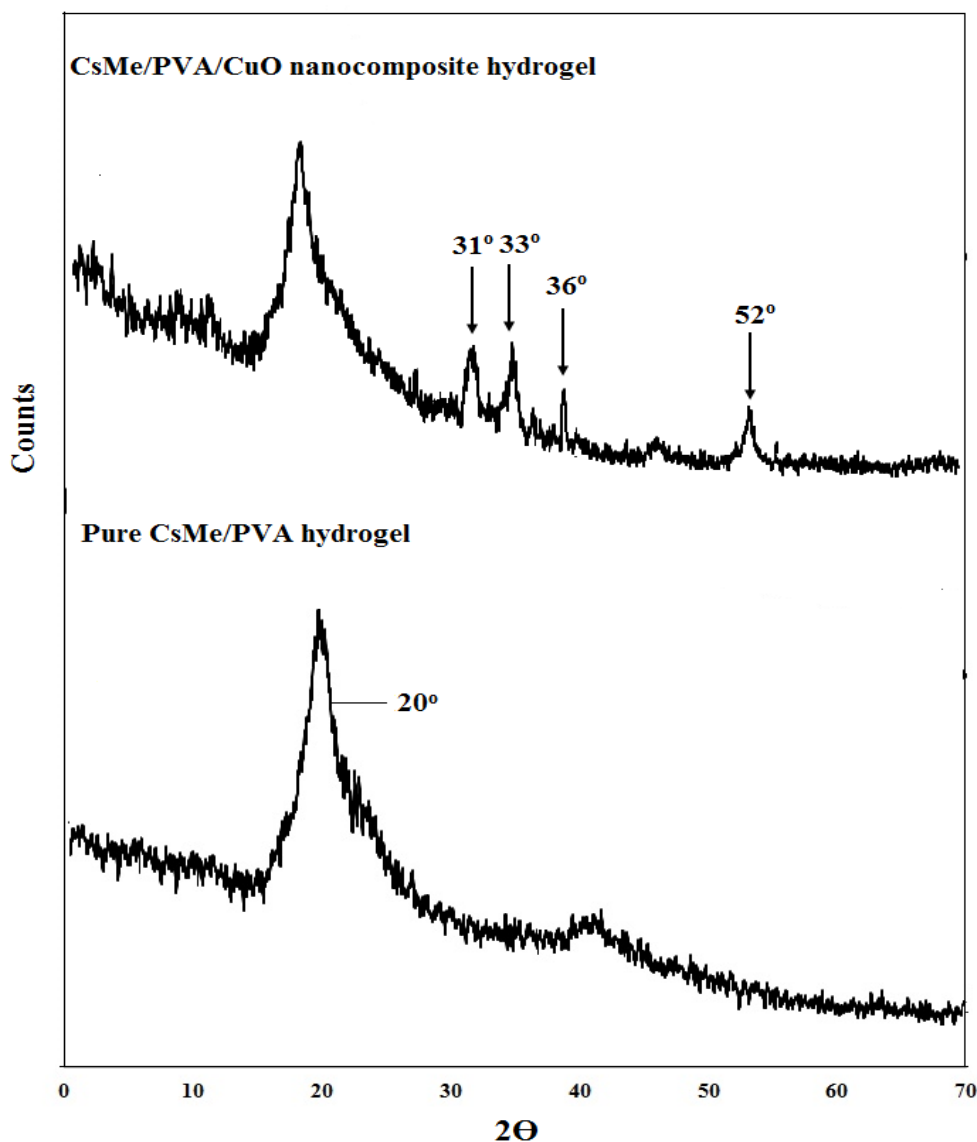
Figure 2: XRD pattern of pure CsMe/PVA hydrogel and CsMe/PVA/CuO nanocomposite hydrogel.
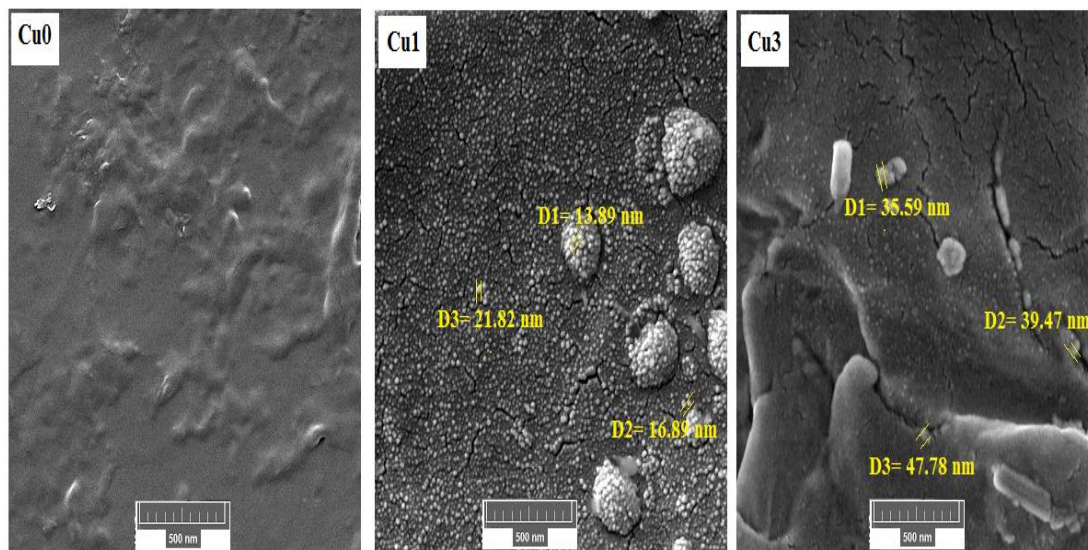
Figure 3: SEM images of pure CsMe/PVA hydrogel (Cu0) and CsMe/PVA/CuO nanocomposite hydrogels with prepared different concentrations of copper chloride: 0.5% and 1.5% (Cu1 and Cu3).

Figure **4** shows the EDX results of CsMe/PVA/CuO nanocomposite hydrogels. The element information and distribution of elements in hydrogel structure were obtained using EDX analysis that indicates the structure of nanocomposite hydrogels contains CuO nanoparticles. Four typical elements on the CsMe/PVA/CuO hydrogels surface are C, O, N, and CuO shown in Figure **4** [29, 36, 37].

Element	Wt. (%)
C	49.80
O	39.92
N	2.43
CuO	7.85
Total	100.00
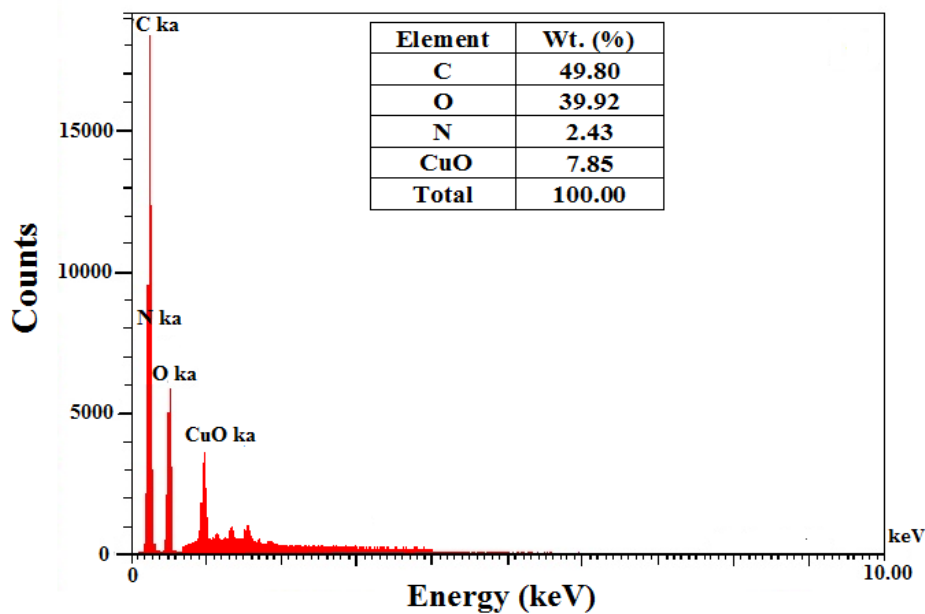
Figure 4: The EDX of (a) CsMe/PVA/CuO nanocomposite hydrogel.

Antibacterial Activity

The in vitro antibacterial properties of CsMe/PVA/CuO nanocomposite hydrogels were tested comparatively against Gram-negative (*E. coli*) and Gram-positive (*S. aureus*) bacteria by disk diffusion test. Inhibition zone under and around the tested samples for bacterial growth was detected visually and listed in Table **1**. The inhibition zones are presented in Figure **5**. The results suggest that the CuO embedded nanocomposite hydrogels revealed a more toxic effect on bacteria than pure hydrogel under similar conditions as evidenced by higher inhibition zone. The antibacterial effect of CsMe/PVA/CuO nanocomposite hydrogels could be associated to the attachment of CuO nanoparticles to the cell wall of bactericides which damages the cell wall and causing leakage of proteins and other intracellular constituents and ultimately causes cell death [38-40]. The results in the Table **1** show that the antibacterial efficiency of the nanocomposite hydrogels is influenced by the concentration of the CuO nanoparticles regardless of the kind of bacterial used. Hydrogels with more CuO nanoparticles demonstrate greater antibacterial properties. From the results, we revealed that CsMe/PVA/CuO nanocomposite hydrogels showed better activity towards Gram-positive bacteria than Gram-negative.

Table 1: Antibacterial activity data of CsMe/PVA/CuO nanocomposite hydrogels against *E. coli* and *S. aureus*.

Sample code	Inhibition Zone (mm)	
	E. coli	*S. aureus*
Cu0	0	0
Cu1	5	9
Cu2	8	13
Cu3	12	17

Effect of pH on swelling behavior

The swelling behavior of the hydrogels was studied in the pH range of 2 to 10 in order to investigate the pH-sensitivity of the prepared hydrogels. As shown in the Figure **6**, the swelling of all the hydrogels increased with the increase of the pH from 2 to 7, however, it decreased at higher pH values (pH> 7). With increasing pH from 2 to 7, carboxyl and hydroxyl groups on the CsMe and PVA chains converted to negatively charged carboxylate and alkolate ions, resulting in higher electrostatic repulsion and water would be taken up [41, 42]. Although we expected to see a rise in the swelling at higher pH values (pH> 7), but a reducing pattern observed. at pH> 7, the higher concentration of Na^+ cations shielded the carboxylate and alkolate ions and preventing complete anion-anion

repulsion and restrain the extending of the tangled molecular chain of the hydrogel [43].

In addition, the results in the Figure **6** show that CuO nanocomposite hydrogels revealed a higher swelling capacity, compared to the neat CsMe/PVA hydrogel. The improvement of the swelling capacity of the CuO nanocomposite hydrogels may be attributed to the presence of CuO nanoparticles with different size, morphology and surface charges. Charged CuO nanoparticles results in the penetration of more water molecules to balance the build-up ion osmotic pressure, which causes the hydrogel to swell [44-46]. Furthermore, formation of CuO nanoparticles in the hydrogel network can expand the hydrogel network and increase the pores and free spaces within the networks and as a consequence adsorbs more water [47, 48].
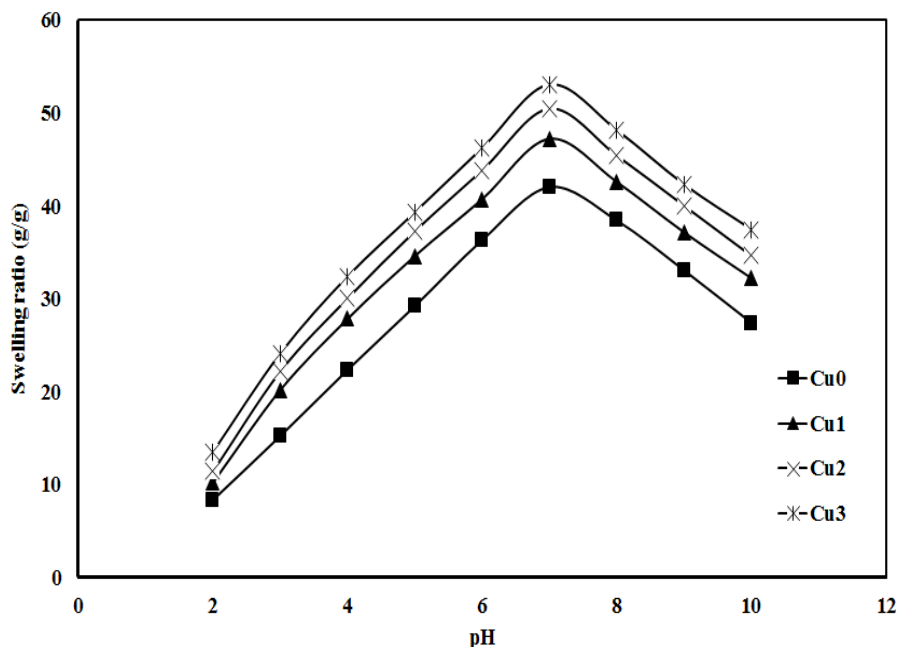
Figure 6: Swelling behavior of CsMe/PVA/CuO nanocomposite hydrogels at different pH values.

Swelling behavior in saline solutions

The swelling of the superabsorbent composite depends on the type and valence of the cations. The equilibrium swelling data obtained from the chloride salt solutions of sodium, calcium and aluminum with

same concentration are given in Figure **7**. As shown, cation charge has a great influence on swelling capacity. As shown in Figure **7**, multivalent cations decrease the swelling capacity considerably. This dramatic decrease in the water absorbency in multivalent cationic solutions could be due to the

complexing ability of the carboxylate groups with multivalent cations. Formation of intramolecular and intermolecular complexes resulted in an increase in the crosslinking density of the network. Therefore, absorbency for the hydrogel in the studied salt solutions is in the order of monovalent > divalent >

trivalent cations. Similar results have been reported in previous studies [49]. According to this Figure CuO nanocomposite hydrogels have rather higher absorbencies in salt solutions in comparison with pure hydrogel.
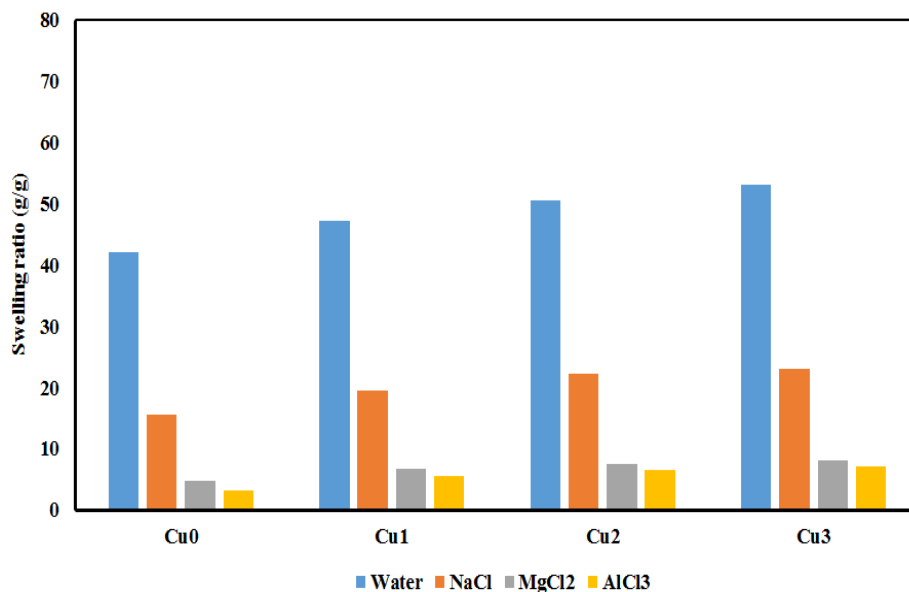
Figure 7. Swelling behavior of CuO nanocomposite hydrogels in different salt cation solutions (the NaCl, $CaCl_2$ and $AlCl_3$ concentrations were chosen 0.2 M).

Conclusion

In this project, antibacterial CsMe/PVA/CuO nanocomposite hydrogels were prepared based on the combination of CuO nanoparticles and biopolymer carboxymethyl chitosan and poly (vinyl alcohol). Pure CsMe/PVA hydrogel and CsMe/PVA/CuO nanocomposite hydrogels were successfully synthesized via crosslinking with ECH in an alkaline medium. Structural details of CsMe/PVA/CuO nanocomposite hydrogels were provided by FT-IR, XRD, EDX and SEM analysis. In addition, their swelling behavior was studied at various pH values and salt solutions. XRD and EDX analysis studies confirmed the formation of CuO nanoparticles in the hydrogel matrix. SEM micrographs clearly showed that CuO nanoparticles with size ranging from 13.89-47.78 nm were formed within the hydrogel matrix, and the number of CuO nanoparticles increased with the increase of Cu^{2+} concentration. The swelling capacity of the CuO nanocomposite hydrogels was dependent on the abundance of the copper oxide nanoparticles in the CsMe/PVA hydrogels. The swelling of the nanocomposite hydrogels increased with increasing the copper chloride concentration and is found to be pH

dependent. Swelling capacity for these hydrogels in salt solutions with the same concentration is in order of NaCl > $CaCl_2$ > $AlCl_3$. Antibacterial activity of the prepared nanocomposite hydrogels was studied against *E. coli* (Gram-negative) and *S. aureus* (Gram-positive) using the agar diffusion test. The results showed an excellent antibacterial activity for CsMe/PVA/CuO nanocomposite hydrogels.

Experimental

Materials

Chitosan (medium molecular weight and viscosity 200-800 cp), Poly (vinyl alcohol) (PVA, molecular mass of 72000), monochloroacetic acid (99%), Epichlorohydrin (ECH, 99.5%), $CuCl_2.H_2O$, NaOH and methanol were purchased from Merck Co. and used as received.

Methods

Preparation of carboxymethyl chitosan

Carboxymethyl chitosan (CsMe) was prepared using the following procedure: 5 g of chitosan was dissolved

in 20% w/v NaOH solution for 15 min. 15 g of monochloroacetic acid was then added drop-wise to the mixture with constant mechanical stirring for 2 h at T=40 ^{o}C until a homogenous mixture was obtained. The obtained mixture was neutralized with 10% acetic acid, poured into an excess of 70% methanol, filtered using a G2 sintered glass funnel, and washed several times with methanol to remove the residual NaOH and monochloroacetic acid. Finally, the obtained CsMe powder was dried in a vacuum oven at T=55 ^{o}C for 8 h.

Preparation of crosslinked CsMe/PVA hydrogels

CsMe powder was first dissolved in 100 ml distilled water containing 3 wt% NaOH at ambient temperature with constant stirring overnight until a clear homogeneous solution was obtained. PVA solution was dissolved in distilled water with continuous stirring at T=95 ^{o}C for 2 h. After cooling at ambient temperature, the CsMe solution was combined with PVA solution by stirring for 2 h in order to obtain a homogenous solution of the two polymers. ECH was used as a crosslinking agent that was added dropwisely to the reaction mixture and stirred for 2 h. Then, the obtained mixture was submerged in a warm water bath at T=80 ^{o}C for 2 h. After collecting the crosslinked CsMe/PVA paste, which is not soluble, it was rinsed using distilled water to remove the residual ECH and NaOH on the hydrogel surface. Lastly, the hydrogel was desiccated in an oven at T=50 ^{o}C for 24 h.

Preparation of CsMe/PVA/CuO nanocomposite hydrogels

As it was explained previously, the nanocomposite hydrogels of CsMe/PVA/CuO was prepared. Normally, 1 g of dry CsMe/PVA hydrogel was submerged in a series of copper chloride solutions with diverse weight ratios (0%, 0.5%, 1% and 1.5%) for 24 h. The Cu ion-loaded hydrogels were washed with distilled water to remove the remaining Cu ions. Then, the hydrogels were immersed in a NaOH solution of 0.2 M for 24 h to oxidation of the bound Cu ions. After washing the hydrogels with distilled water, the resulting products were dried in an oven at T=50 ^{o}C for 24 h. The CsMe/PVA/CuO nanocomposite hydrogels with 0%, 0.5%, 1% and 1.5% $CuCl_2$ are referred to as Cu0, Cu1, Cu2, and Cu3, respectively.

Antibacterial activity

Antibacterial experiments were studied against both *S. aureus* (Gram-positive) and *E. coli* (Gram-negative) bacteria by agar diffusion test. For agar diffusion method, samples exposed to bacteria in solid media (nutrient agar), and the inhibition zone around samples was determined as the antibacterial effect of CuO nanoparticles. The agar plates were inoculated with 100 μL spore suspensions of bacteria. The swelled hydrogels, each of which contained test materials at the same size were cut and placed on the agar plate, then incubated with bacterial suspension at 37°C for 24 h.

Swelling behavior

Swelling ratio of CsMe/PVA/CuO nanocomposite hydrogels were measured according to the previously reported methods. 0.1 g of powdered CsMe/PVA/CuO nanocomposite hydrogels were immersed in 50 ml of aqueous solutions with desired pH at room temperature for 24 h to reach maximum swelling equilibrium. The swelling ratio of nanocomposite hydrogels was determined according to Equation 1.

Swelling ratio (SR%) = W_2 – W_1/W_1 × 100 Eq. (1)

Where W_1 is initial weight of sample, and W_2 is the weight of the sample after swelling for 24 h. To prepare the pH media, standard HCl (1.0 M) and NaOH (1.0 M) solutions were diluted with distilled water to reach the desired acidic and basic pHs, respectively.

The water absorbency of the hydrogels in aqueous solutions of the salts (0.2M of NaCl, $CaCl_2$, and $AlCl_3$) was determined in a similar manner.

Characterization and analysis

Infrared spectra was recorded on a FT-IR spectrometer (Bruker Instruments, model Aquinox 55, Germany) in the wave number ranging 4000-400 cm^{-1} at a resolution of 0.5cm^{-1} as KBr pellets. The X-ray diffraction pattern of the samples were verified with Siemens-D500 diffractometer using Cu-kα radiation at 35 kV in the scan range of 2θ from 2 to 70° and scan rate of 1°/min. All of analyzed samples were in powdery form. The morphology of the dried neat hydrogel and nanocomposite hydrogels was examined by scanning electron microscope (SEM) (TESCAN MIRA) after coating the dried hydrogels with gold and silver films. To verify the CuO distribution in the CsMe/PVA/CuO nanocomposite hydrogels matrix, energy dispersive X-ray spectroscopy (EDX) was applied.

References

[1] Gholamali, I.; Hosseini, S. N.; Alipour, E.; Yadollahi, M. *Starch/Stärke.,* **2019**, *71*, 3-4.

[2] Ullah, F.; Othman, M. B. H.; Javed, F.; Ahmad, Z.; Akil, H. M. *Mater. Sci. Eng. C.,* **2015**, *57*, 414.

[3] Wu, T.; Li, Y.; Lee, D. S. *Macromol. Res.*, **2017**, *25(6)*, 480.

[4] Namazi, H.; Rakhshaei, R.; Hamishehkar, H.; Samadi Kafil, H. *Inter. J. Biol. Macromol.,* **2016**, *85*, 327.

[5] Park, S. A.; Lee, S. H.; Kim, W. D. *Macromol. Res.,* **2011**, *19(7)*, 694.

[6] Van Vlierberghe, S.; Dubruel, P.; Schacht, E. *Biomacromolecules.*, **2011**, *12*, 1387.

[7] Hoare, T. R.; Kohane, D. S. *Polym.,* **2008**, *49*, 1993.

[8] Yadollahi, M.; Namazi, H. *J. Nanopart. Res.,* **2013**, *15*, 1563.

[9] Wahid, F.; Yin, J. J.; Xue, D. D.; Xue, H.; Lu, Y. S.; Zhong, C.; Chu, L. Q. *Inter. J. Biol. Macromol.,* **2016**, *88*, 273.

[10] Bai, X.; Bao, Z.; Bi, S.; Li, Y.; Yu, X.; Hu, S.; Tian, M.; Zhang, X.; Cheng, X.; Chen, X. *Macromol. Biosci.,* **2018**, *18*, 3.

[11] Khan, S.; Akhtar, N.; Minhas, M. U.; Badshah, S. F. *AAPS PharmSciTech.*, **2019**, *20*, 119.

[12] Mohamed, R. R.; Sabaa, M. W. Inter. *J. Biol. Macromol.,* **2014**, *69*, 95.

[13] Upadhyaya, L.; Singh, J.; Agarwal, V.; Pandey, A. C.; Verma, S. P.; Das, P.; Tewari, R. P. *Process. Biochem.,* **2015**, *50*, 678.

[14] Wahid, F.; Wang, H. S.; Lu, Y. S.; Zhong, C.; Chu, L. Q. *Inter. J. Biol. Macromol.*, **2017**, *101*, 690.

[15] Upadhyaya, L.; Singh, J.; Agarwal, V.; Tewari, R. P. *Carbohyd. Polym.,* **2013**, *91*, 452.

[16] Upadhyaya, L.; Singh, J.; Agarwal, V.; Tewari, R. P. *J. Control. Release.,* **2014**, *186*, 54.

[17] Riedo, C.; Caldera, F.; Poli, T.; Chiantore, O. *Harit. Sci.,* **2015**, *3*, 33.

[18] Ranjha, N. M.; Khan, S. J. *Pharm. Altern. Med.,* **2013**, *2*, 30.

[19] Zhao, L.; Mitomo, H.; Zhai, M.; Yoshii, F.; Nagasawa, N.; Kume, T. *Carbohyd. Polym.*, **2003**, *53*, 439.

[20] Ahmadian, Y.; Bakravi, A.; Hashemi, H.; Namazi, H. *Polym. Bull.,* **2018**, *76*, 1967.

[21] Sabaa, M. W.; Abdallah, H. M.; Mohamed, N. A.; Mohamed, R. R. *Mat. Sci. Eng. C.,* **2015**, *56*, 363.

[22] Agnihotri, S.; Mukherji, S.; Mukherji, S. *Appl. Nanosci.,* **2012**, *2*, 179.

[23] Malmsten, M. *Soft Matter.,* **2011**, *7*, 8725.

[24] Sharma, V. K.; Yngard, R. A.; Lin, Y. *Adv. Colloid. Interfac.,* **2009**, *145(1)*, 83.

[25] Juby, K. A.; Dwivedi, C.; Kumar, M.; Kota, S.; Misra, H. S.; Bajaj, P. N. *Carbohyd. Polym.,* **2012**, *89*, 906.

[26] Reddy, P. R.; Varaprasad, K.; Sadiku, R.; Ramam, K.; Reddy, G. V. S.; Raju, K. M.; Reddy, N. S. *J. Inorg. Organomet. P.,* **2013**, *23*, 1054.

[27] Varaprasad, K.; Mohan, Y. M.; Vimala, K.; MohanaRaju, K. *J. App. Polym. Sci.,* **2011**, *121*, 784.

[28] Hebeish, A.; Hashem, M.; Abd El-Hady, M. M.; Sharaf, S. *Carbohyd. Polym.,* **2013**, *92*, 407.

[29] Khorasani, M. T.; Joorabloo, A.; Moghaddam, A.; Shamsi, H.; Mansoori Moghadam, Z. *Inter. J. Biol. Macromol.,* **2018**, *114*, 1203.

[30] Song, F.; Li, X.; Wang, Q.; Liao, L.; Zhang, C. *J. Biomed. Nanotechnol.,* **2015**, *11*, 40.

[31] Gholamali, I.; Asnaashariisfahani, M.; Alipour, E. *Regen. Eng. Transl. Med.,* **2019**, 1.

[32] Rasoulzadeh, M.; Namazi, H. *Carbohyd. Polym.,* **2017**, *168*, 320.

[33] Mohamadnia, Z.; Zohuriaan-Mehr, M. J.; Kabiri, K.; Razavi-Nouri, M. *J. Polym. Res.,* **2008**, *15*, 173.

[34] Yadollahi, M.; Gholamali, I.; Namazi, H.; Aghazadeh, M. *Inter. J. Biol. Macromol.,* **2015**, *74*, 136.

[35] Barkhordari, S.; Yadollahi, M.; Namazi, H. *J. Polym. Res.,* **2014**, *21(6)*, 1.

[36] Zare-Akbari, Z.; Farhadnejad, H.; Furughi-Nia, B.; Abedin, S.; Yadollahi, M.; Khorsand-Ghayeni, M. *Inter. J. Biol. Macromol.,* **2016**, *93*, 1317.

[37] Rasoulzadehzali, M.; Namazi, H. *Inter. J. Biol. Macromol.,* **2018**, *116*, 54.

[38] Ingle, A. P.; Duran, N.; Rai, M. *Appl. Microbial. Bio.,* **2013**, 1.

[39] Das, D.; Nath, B. C.; Phukon, P.; Dolui, S. K. *Colloid. Surface. B.,* **2013**, *101*, 430.

[40] Gopalakrishnan, K.; Ramesh, C.; Ragunathan, V.; Thamilselvan, M. *Dig. J. Nanomater. Bio.,* **2012**, *7(2)*, 833.

[41] Zakhireh, S.; Mahkam, M.; Yadollahi, M.; Jafarirad, S. *J. Polym. Res.,* **2014**, *21*, 1.

[42] Pourjavadi, A.; Ghasemzadeh, H.; Soleyman, R. *J Appl Polym Sci.* **2007**, *105*, 2631.

[43] Shariatinia, Z. *Inter. J. Biol. Macromol.,* **2018**, *120*, 1406.

[44] Gils, P. S.; Ray, D.; Sahoo, P. K. *Inter. J. Biol. Macromol.,* **2010**, *46*, 237.

[45] Vimala, K.; Samba Sivudu, K.; Murali Mohan, Y.; Sreedhar, B.; MohanaRaju, K. *Carbohyd. Polym.,* **2009**, *75*, 463.

[46] Xiang, Y.; Chen, D. *Eur. Polym. J.,* **2007**, *43*, 4178.

[47] Jayaramudu, T.; Raghavendra, G. M.; Varaprasad, K.; Sadiku, R.; Ramam, K.; Raju, K. M. *Carbohyd. Polym.,* **2013**, *95*, 188.
[48] Jayaramudu, T.; Raghavendra, G. M.; Varaprasad, K.; Sadiku, R.; Raju, K. M. *Carbohyd. Polym.,* **2013**, *92*, 2193.
[49] Yadollahi, M.; Gholamali, I.; Namazi, H.; Aghazadeh, M. *Inter. J. Biol. Macromol.,* **2015**, *73*, 109.